ELSEVIER

Computational Materials Science 6 (1996) 158–172

COMPUTATIONAL MATERIALS SCIENCE

Review of atomistic simulations of surface diffusion and growth on semiconductors

Efthimios Kaxiras

Department of Physics and Division of Applied Sciences, Harvard University, Cambridge, MA 02138, USA

Abstract

Recent experimental work on surface diffusion and growth phenomena on semiconductors has inspired a number of atomistic simulations. These are based either on empirical approaches such as classical interatomic potentials, or on first-principles quantum mechanical calculations. After a brief overview of relevant experimental work, we review the basic features of the theoretical approaches and discuss their advantages and shortcomings in the context of surface diffusion and growth simulations for semiconductors. Some representative systems, for which calculations employing different computational approaches have been reported in the literature, are discussed in detail.

1. Introduction

In the last few years the need to *understand* and *control* the properties of solids at the microscopic level and with chemical specificity has increased substantially. This is driven by the demands of technology, including smaller and faster computer chips, efficient and reliable solid-state lasers at various wavelengths, ultra-hard composites that can withstand high temperatures, etc. For many of these applications, it is essential to understand the effects of specific atomic-scale features on the properties of real solids. This represents a challenge for existing theoretical approaches (for an interesting perspective on the theory of materials and its relevance to technological applications see [1]).

In the field of semiconductors, interest in growth phenomena has exploded in recent years, in the hope that through careful control of growth the production of a wide range of new optical and electronic devices will become feasible. Remarkable advances in experimental techniques, which for the first time provided clues on the atomistic mechanisms of growth, have increased interest in microscopic theories. While the present paper is concerned mostly with the theoretical aspects of modeling semiconductor growth phenomena, we begin with a short discussion of relevant experimental work as an introduction to some important issues. The discussion of experiments is not exhaustive; rather, it is intended as a rough tour guide to a fascinating landscape, seen through the lens of the author's interests, and beckoning the reader to further exploration.

A central issue in growth phenomena is the diffusion of atoms deposited on a substrate. The first direct measurements of atomic diffusion on semiconductor surfaces were provided by the scanning tunneling microscopy (STM) experiments of Lagally and coworkers on Si(100) surfaces [2]. This work established the crucial link between surface reconstruction and the dynamics of atoms on semiconductor surfaces, by showing that the rate of diffusion in the two inequivalent directions on this surface differs by three orders of magnitude: the direction of fast

0927-0256/96/$15.00 Copyright © 1996 Elsevier Science B.V. All rights reserved.
PII S0927-0256(96)00030-4

motion is along the rows of dimers, which form the reconstruction pattern on this surface. Further experimental work by the same group revealed the importance of steps, and the dependence of their stability on dimer orientation [3]. These authors also demonstrated the effect of the substrate on features of hetero-epitaxial islands: the intriguing shape of Ge islands grown on Si(100) substrates and the reconstructions on their exposed faces [4], which are not normally observed on native Ge surfaces, remain an unexplained and poorly understood manifestation of the importance of atomistic processes in growth phenomena.

Surface diffusion, step motion and the interplay between surface structure and dynamical phenomena was demonstrated for the Si(111) surface by the STM work of Williams and coworkers [5]. In contrast to Si(100), the Si(111) surface is isotropic and the reconstruction is based on a periodic pattern of adatoms, as well as certain other features such as dimerization, corner holes and the presence of a stacking fault in one half of the unit cell [6]. The standard reconstruction pattern has a (7×7) periodicity, although on surfaces that have been annealed and quenched, periodicities ranging from (5×5) to (11×11) are also observed, as well as reconstructions with a higher density of adatoms [such as (2×2) and $(\sqrt{3} \times \sqrt{3})$]. On the structurally similar Ge(111) surface, which exhibits an adatom pattern with $c(2 \times 8)$ periodicity, STM studies by Golovchenko and coworkers [7] measured a diffusion constant which is many orders of magnitude lower than anticipated from simple estimates and standard numbers for the attempt frequency and the hopping length; these effects have been successfully explained through first-principles calculations and Monte Carlo simulations by Kaxiras and Erlebacher [8].

Direct observation of dynamical phenomena such as step motion has become feasible through a relatively new and powerful experimental technique, low-energy electron microscopy (LEEM). Tromp and coworkers [9] and Williams and coworkers [10] have presented real-time images of step motion on Si(100) and Si(111) surfaces, including the effects of adsorbates.

Experiments on the nature of growth on compound semiconductors have been reported by Orr and coworkers [11], using STM and atomic force microscopy (AFM) over very large areas. Through these studies, a convincing link has been established between the microscopic features of the surface and the macroscopic nature of growth: the presence of island-edge barriers to downhill diffusion (often referred to as 'Erlich–Schwoebel' barriers), was invoked to explain the formation of gently slopped mounds on GaAs(100) surfaces, which lead to surface roughening. While successful analytic treatments of this effect have already been developed [12,13], the details of atomistic structure and diffusion pathways that give rise to the island-edge barriers remain unclear and deserve further investigation by theoretical modeling. Work along these lines has recently been reported for Al surfaces [14].

One of the most challenging aspects of heteroepitaxial growth is the effect of strain. The transmission electron microscopy (TEM) work of LeGoues and coworkers [15] has described in detail the structure of dislocations at the interface between the substrate and the strained overlayers in the Si/Ge system. For the same system, TEM work by Jesson, Pennycook and coworkers, has revealed a variety of possible ordering schemes [16]. Models that attempt to explain these phenomena, using either thermodynamic or kinetic arguments, have been considered in the preceding references.

Ordering phenomena have also been the subject of much experimental and theoretical work on compound semiconductor surfaces [17]. An recent review of the subject, discussing both the experimental and theoretical approaches, has been provided by Zunger and Mahajan, to which we refer the interested reader [18]. Briefly, it is worth noting that surface structure is believed to play an important role in such phenomena. In particular, the surface reconstruction introduces a pattern of strain to substrate sites, which is responsible for the observed ordering patterns. The same effect of surface structure on atomic ordering has been discussed by Kelires and Tersoff for the Si/Ge system [19].

On a different front, Copel et al. were the first to report attempts to control and manipulate the growth mechanisms in heteroepitaxy using surfactants [20]. These experiments represent some of the most intriguing and exciting manifestations of the interplay between lattice strain and chemistry on semiconduc-

tor surfaces, and have inspired theoretical investigations of the microscopic nature of the surfactant mechanism [21–23], as well as macroscopic treatments of the phenomenon [24]. More recently, surfactants have been used to improve and control both homoepitaxial and heteroepitaxial growth of various elemental and compound semiconductors [25–32].

2. Overview of theoretical approaches

The surface growth phenomena mentioned above ieed to be studied theoretically, using both analytical ipproaches where the microscopic details are not :xplicitly present, as well as computational ap-)roaches where the atomistic structure and the dy- iamics of atoms are the central theme. Here we will :oncentrate on methodologies that allow the study of nicroscopic phenomena. The emphasis will be on he different methods for describing the interactions ›etween atoms, rather than on the general schemes or describing the time evolution of a system once he atomic interactions have been specified (such as nolecular dynamics or Monte Carlo). Detailed de- criptions of these schemes are available in text- ooks [33] and the domains of applicability of each iethod are well understood. In contrast, the advan- iges and disadvantages of different approaches to escribe atomic interactions are still under investiga- on. There is a hierarchy of such methods, ranging ·om classical interactions, to empirical quantum me- ianical calculations, to fully self-consistent quan- im mechanical calculations. Conceptually and com- utationally, the simplest description of the atomic iteractions is through a classical potential function. lethods that include an explicit, quantum mechani- il treatment of the valence electrons of a solid are .ore realistic, but also more computationally de- anding; it is after all the presence of these electrons at determines the interaction among ions in a solid. 'e shall describe representative methods of each pe in the following.

1. Classical interactions: the case of Si

In physical systems where the ions are bonded edominantly by covalent interactions with strong eference for particular bond angles, as is the case in most semiconductors, a simple two-body interatomic potential is not adequate. Three-body or higher order terms, or more complicated expressions that are functions of the local atomic environment, are required. Much effort has been devoted to producing a many-body interatomic potential for silicon, the prototypical covalently bonded solid and semiconductor [34–46]. As the extensive literature on the subject demonstrates, capturing the physics of covalent bonding by a classical interatomic potential is difficult. It is perhaps overly optimistic to expect that a single classical potential will be able to describe accurately all aspects of an inherently quantum mechanical phenomenon, such as the formation of electronic bonds between the ions in a solid. Nevertheless, the above classical potentials for Si have been used extensively in the literature to study phenomena that cannot be handled by quantum mechanical methods. Indeed, when these potentials are used in a proper manner (a notion to be elaborated on in the next section), they can be powerful tools for describing complex systems.

In order to provide an idea of what is involved in a typical Si interatomic potential, we briefly describe the two most popular ones, the Stillinger and Weber [36] and the Tersoff [38] classical potentials. These two models represent somewhat different philosophies in the classical potential approach. In the Stillinger–Weber potential, the total energy of a system of atoms is given as an expansion in n-body terms, with the series cut off at some order n (here $n = 3$ and the one-body term is set to zero):

$$E = \sum_{i<j} V_2(i, j) + \sum_{i<j<k} V_3(i, j, k). \quad (1)$$

The two-body potential $V_2(i, j)$ depends only on the distance r_{ij} between neighbors labeled i and j:

$$V_2(i, j) = v(r_{ij}), \quad (2)$$

$$v(r) = A(Br^{-p} - r^{-q})\exp\left[(r-a)^{-1}\right]. \quad (3)$$

The three-body potential $V_3(i, j, k)$ depends on the distances r_{ij}, r_{jk}, r_{ki}, as well as the angles θ_{ijk}, θ_{jki}, θ_{kij} subtended by these distances, for the triplet of neighbors labeled i, j and k:

$$V_3(i, j, k) = u(r_{ij}, r_{ik}, \theta_{ijk}) + u(r_{jk}, r_{ji}, \theta_{jki}) + u(r_{ki}, r_{kj}, \theta_{kij}), \quad (4)$$

$$u(r_{ij}, r_{ik}, \theta_{ijk}) = \lambda \exp\left[\gamma(r_{ij}-a)^{-1} + \gamma(r_{ik}-a)^{-1}\right] \times \left(\cos\theta_{ijk} + \tfrac{1}{3}\right)^2. \quad (5)$$

Pairs of atoms are considered neighbors when their distance is shorter than a cutoff radius a (the variable that appears in the above equations); otherwise the two-body and three-body terms vanish. All the parameters in these equations are fitted to reproduce certain important physical properties of bulk Si, such as the optimal bond length and cohesive energy of the lowest-energy crystal structure of Si (the diamond lattice), and its melting point.

In contrast to this approach, the Tersoff potential consists of a sum over two-body interactions, each of which depends on its local environment:

$$E = \tfrac{1}{2} \sum_{i \neq j} V_{ij}, \quad (6)$$

$$V_{ij} = f_C(r_{ij})\left[a_{ij} f_R(r_{ij}) + b_{ij} f_A(r_{ij})\right], \quad (7)$$

where all pairs of atoms ij are identified as neighbors through a cutoff function $f_C(r)$ which is 1 for $r < R - D$, 0 for $r > R + D$ and falls smoothly from 1 to 0 for $R - D < r < R + D$, as

$$f_C(r) = \frac{1}{2} - \frac{1}{2}\sin\left[\frac{\pi(r-R)}{2D}\right]. \quad (8)$$

The functions $f_R(r)$ and $f_A(r)$ are exponentially decaying functions:

$$f_R(r) = A\exp(-\lambda_1 r), \quad (9)$$

$$f_A(r) = -B\exp(-\lambda_2 r). \quad (10)$$

The quantities a_{ij} and b_{ij} represent bond length and bond angle terms, that involve a dependence on the environment:

$$a_{ij} = \left(1 + \alpha^n \eta_{ij}^n\right)^{-1/2n}, \quad (11)$$

$$\eta_{ij} = \sum_{k \neq i,j} f_C(r_{ik}) \exp\left[\lambda_3^3 (r_{ij} - r_{ik})^3\right], \quad (12)$$

$$b_{ij} = \left(1 + \beta^n \zeta_{ij}^n\right)^{-1/2n}, \quad (13)$$

$$\zeta_{ij} = \sum_{k \neq i,j} f_C(r_{ik})\, g(\theta_{ijk}) \exp\left[\lambda_3^3 (r_{ij} - r_{ik})^3\right], \quad (14)$$

$$g(\theta) = 1 + \frac{c^2}{d^2} - \frac{c^2}{d^2 + (h - \cos\theta)^2}. \quad (15)$$

The environment dependence comes through the summation over all other neighbors $k \neq i$, j that appear in the terms η_{ij} and ζ_{ij}, where θ_{ijk} is the angle subtended by the bonds r_{ij} and r_{ik}. As in the case of the Stillinger–Weber potential, the parameters of the Tersoff potential are chosen so that it reproduces important physical properties, such as the binding energy of the dimer, the bond energy and lattice constant of several bulk forms of Si, elastic properties, etc. In the case of the Tersoff potential, the underlying many-body expansion is not truncated at any order; rather, terms of all orders are included in some undetermined combination. This is evident from the fact that the two-body term includes all neighbors of each pair of atoms. In this sense, the Tersoff potential is a true many-body potential.

Both the Stillinger–Weber and the Tersoff potentials include of order 10 free parameters. This is also the case for most other potentials for Si, which in general are similar to the two representative potentials described above, i.e. they are either an explicit two- and three-body (or higher order) truncation of a many-body expansion, or an implicit effective many-body potential in which the pair or higher order terms include a dependence on the local environment.

2.2. *Empirical quantum mechanical calculations: the tight-binding approximation*

The next level of sophistication in treating atomic interactions in solids is the tight-binding approximation. In this approach, electronic degrees of freedom are explicitly present, but the electron wavefunctions are not determined self-consistently. Rather, the hamiltonian matrix elements between atomic-like electron orbitals are chosen to have fixed values (typically including a distance dependence) [47]. The electron interactions are then taken into account by diagonalizing the hamiltonian for each atomic configuration, which at least contains some level of description of rehybridization effects when the relative orientations of bonds change. The sum of the eigenvalues of the hamiltonian represents an impor-

tant contribution to the total energy of the solid, arising from changes in the electronic density as the atomic structure evolves. This, however, is not sufficient to describe all the changes in the total energy of the solid, and additional terms need to be included. One of the earliest attempts to provide such a complete scheme is due to Chadi [48]; this was followed by several refinements and improvements [49–57]. We briefly outline here one of these schemes, as a representative tight-binding formulation [51]. The total energy is written as:

$$E = 2\sum_{i=1}^{2N} (\varepsilon_i - \varepsilon_0) + E_2 + E_3 + E_4, \quad (16)$$

where the first term is the sum of $2N$ eigenvalues of the hamiltonian that correspond to occupied electronic states, each containing two electrons (due to spin degeneracy); the eigenvalues are given with respect to a reference value ε_0. The remaining terms provide the necessary corrections to produce a reasonable total-energy expression: The second term is:

$$E_2 = \sum_{l=2}^{N} \sum_{l'=1}^{l-1} E_r(|\boldsymbol{R}_l - \boldsymbol{R}_{l'}|), \quad (17)$$

where $\boldsymbol{R}_l$ denotes the position of ion l and E_r is a repulsive energy term that vanishes beyond a cutoff distance R_b, through a smooth cutoff function (for example, similar to the one discussed in connection with the Tersoff classical potential). This term is needed to neutralize the effect of double-counting the Coulomb and exchange-correlation interactions in the band structure term, since the energies ε_i are obtained from single-particle equations. The third term is a polynomial in n_b/N,

$$E_3 = N\sum_{i=0}^{2} \alpha_i \left(\frac{n_b}{N}\right)^i, \quad (18)$$

where n_b is the number of bonds, determined by a sum of a cutoff function over all pairs of atoms (the same cutoff function as in E_2 can be used). This term is needed to avoid favoring highly-coordinated structures. Finally, the last term is

$$E_4 = U\sum_{l=1}^{N} (q_l - q_l^0)^2. \quad (19)$$

In this term, q_l is the charge associated with atom l, calculated from the coefficients of the atomic orbitals that correspond to this atom (which are obtained from the diagonalization of the hamiltonian) and q_0^l is the natural valence of atom l. This term accounts for charge transfer effects. In this formulation there appear several parameters, which are again fixed to reproduce important physical properties such as bond-lengths and bond-angles of representative bulk structures and finite-size structures. Certain parameters, such as the on-site and nearest-neighbor hamiltonian matrix elements, can be taken directly from fits to the band structure of the solid (for example, from the work of Harrison [47]).

2.3. First-principles quantum mechanical calculations

The next step in the treatment of atomic interactions would be to solve self-consistently the true many-body Schrödinger equation for a system of electrons and ions:

$$\mathscr{H}\Psi(\boldsymbol{R}_l; \boldsymbol{r}_i) = E\Psi(\boldsymbol{R}_l; \boldsymbol{r}_i) \quad (20)$$

where $\mathscr{H} = \mathscr{T} + \mathscr{V}$ is the hamiltonian of the system, containing the kinetic energy $\mathscr{T}$ and the potential energy $\mathscr{V}$ due to ion–ion, electron–ion and electron–electron interactions. In the above equations E is the energy of the system and $\Psi(\boldsymbol{R}_l; \boldsymbol{r}_i)$ is the many-body wavefunction that describes the state of the system, with $\boldsymbol{R}_l$ denoting the positions of the ions and $\boldsymbol{r}_i$ denoting the electronic degrees of freedom. Typically, we can assume that the electrons respond instantaneously to any ionic motion due to the large difference in the respective masses, so that the many-body wavefunction Ψ has an explicit dependence on the electronic degrees of freedom alone (this is known as the Born–Oppenheimer approximation). The ions can then be treated as classical particles obeying Newtonian equations of motion. In certain cases, most notably when very light ions (like hydrogen) are present in the system, this approximation is not adequate, and more elaborate methods need to be employed to describe the ionic motion, such as path integral Monte Carlo (see for example, the application to solid hydrogen, by Kaxiras and Guo [58] and references to related work therein). Even within the Born–Oppenheimer approximation, however, solving for $\Psi(\boldsymbol{r}_i)$ is an extremely difficult task, because of the exchange and correlation proper-

ties of electrons. For problems involving more than very few ions and their electrons, exact solutions of Eq. (20) are intractable.

One approach which makes the problem tractable relies on the Density Functional Theory (DFT) of Hohenberg and Kohn [59], which casts the problem in terms of the electronic density $\rho(\boldsymbol{r})$, rather than in terms of the many-body wavefunction:

$$E[\rho(\boldsymbol{r})] = F[\rho(\boldsymbol{r})] + \int \mathrm{d}\boldsymbol{r} V_{\text{ion}}(\boldsymbol{r}) \rho(\boldsymbol{r}). \qquad (21)$$

E is again the total energy of the system of interacting electrons and ions, $F[\rho(\boldsymbol{r})]$ is a universal functional of the density for a system where only Coulomb interactions exist, and V_{ion} is the external potential that every electron experiences due to the presence of the ions. The universal functional $F[\rho(\boldsymbol{r})]$ can be split into three terms, the kinetic energy part $T[\rho(\boldsymbol{r})]$, the Coulomb interaction part $U[\rho(\boldsymbol{r})]$ that represents the repulsion between electrons, and the exchange-correlation part $E_{\text{XC}}[\rho(\boldsymbol{r})]$, that represents the many-body aspects of the interacting electron system. Of these terms, only the Coulomb interaction part has an analytic expression:

$$U[\rho(\boldsymbol{r})] = \frac{1}{2} \iint \mathrm{d}\boldsymbol{r}\, \mathrm{d}\boldsymbol{r}' \frac{\rho(\boldsymbol{r}) \rho(\boldsymbol{r}')}{|\boldsymbol{r} - \boldsymbol{r}'|}. \qquad (22)$$

As proposed by Kohn and Sham [60], the real system of ions and interacting electrons can be mapped onto a system of non-interacting fictitious particles that have exactly the same density as the real electrons. These particles experience an effective potential due to the presence of the ions and the collective potential of all other fictitious particles. A variational calculation leads to a set of single-particle equations for the Kohn–Sham wavefunctions, which must be solved self-consistently, that is, the effective potential appearing in the single particle equations contains the density of the fictitious particles which is given as a sum over the magnitude of the particles' wavefunctions:

$$\left[-\frac{\hbar^2}{2m} \nabla^2 + V_{\text{eff}}(\boldsymbol{r}, \rho(\boldsymbol{r})) \right] \phi_i(\boldsymbol{r}) = \varepsilon_i \phi_i(\boldsymbol{r}), \qquad (23)$$

$$V_{\text{eff}}(\boldsymbol{r}, \rho(\boldsymbol{r})) = V_{\text{ion}}(\boldsymbol{r}) + \int \mathrm{d}\boldsymbol{r}' \frac{\rho(\boldsymbol{r}')}{|\boldsymbol{r} - \boldsymbol{r}'|} + \frac{\delta E_{\text{XC}}}{\delta \rho}, \qquad (24)$$

$$\rho(\boldsymbol{r}) = \sum_{i=1}^{N} |\phi_i(\boldsymbol{r})|^2. \qquad (25)$$

Despite this self-consistency constraint, it is enormously simpler to deal with a set of single-particle equations than with the many-body wavefunction of a fully interacting system.

An important term in the effective potential which every Kohn–Sham fictitious particle experiences comes from a functional derivative of the exchange and correlation density functional $(\delta E_{\text{XC}})/(\delta \rho)$. This term does not have a simple analytical expression in the electronic density, and is inherently non-local. In order to obtain an explicit form, $E_{\text{XC}}[\rho(\boldsymbol{r})]$ is usually approximated by a local functional of the electronic density, an approach known as the Local Density Approximation (LDA):

$$E_{\text{XC}}^{\text{LDA}}[\rho(\boldsymbol{r})] = \int \mathrm{d}\boldsymbol{r}\, \rho(\boldsymbol{r}) v_{\text{XC}}(\rho), \qquad (26)$$

where $v_{\text{XC}}(\rho)$ is a simple analytical function of ρ. This is an unjustified, ad-hoc approximation. Once the LDA approximation has been adopted, the exchange-correlation density functional $v_{\text{XC}}(\rho)$ can be uniquely determined by comparison to quantum Monte Carlo calculations for a homogeneous electron gas, which provide an essentially exact treatment of that simplified system [61].

Recently, much theoretical work has been devoted to improving the accuracy of the exchange-correlation functional by adding corrections that include gradients of the electronic density; these methods are referred to as the Generalized Gradient Approximation or GGA [62]. These corrections are indeed helpful in cases where a vacuum interface is involved (see, for instance, the application to activated adsorption by Hammer et al. [63]), but may not yet be appropriate for universal use (see for example the detailed investigations of the GGA on bulk properties of solids by Juan and Kaxiras [64]).

A useful simplification of the computations comes from the fact that only the valence electrons need to be explicitly considered in solids, while the core electrons of the ions can essentially be integrated out by the use of pseudopotentials [65,66]. A pseudopotential is an effective potential constructed at the level of the atom, which incorporates the effect of the core electrons and produces simplified nodeless wavefunctions for the valence electrons, that have the correct behavior in the regions between the atomic cores.

Once the electronic density has been calculated for a given ionic configuration, the forces on the ions can be obtained through the Hellmann–Feynman theorem. The calculation of the forces permits either full optimization of the structure or molecular dynamics simulation of the ionic motion.

A recent advance, due to Car and Parrinello [67], is based on simultaneous optimization of electronic and ionic degrees of freedom. This is achieved by constructing a Lagrangian, in which the single-particle wavefunctions $\phi_i(\boldsymbol{r})$ of the Kohn–Sham equations are assigned fictitious masses μ and the total energy $E[\{\boldsymbol{R}_{I=1,N_i}\}]$ of the system plays the role of the potential energy in the Lagrangian:

$$\mathscr{L} = \sum_{i=1}^{N_e} \frac{1}{2}\mu\left[\frac{\mathrm{d}\phi_i(\boldsymbol{r})}{\mathrm{d}t}\right]^2 + \sum_{I=1}^{N_i} \frac{1}{2} m_I \left[\frac{\mathrm{d}\boldsymbol{R}_I}{\mathrm{d}t}\right]^2 - E\left[\left\{\boldsymbol{R}_{I=1,N_i}\right\}\right]. \tag{27}$$

In the above equation N_e is the total number of electrons in the system and N_i is the total number of ions. This formulation leads to coupled equations of motion for the electronic and ionic degrees of freedom. Considerably more effective molecular dynamics simulations can be performed in this manner, because for small enough time steps the electronic wavefunctions need not be recomputed self consistently after each ionic displacement, but can be obtained by a time evolution since they are treated as classical variables. A variant of the Car–Parrinello approach incorporates a conjugate gradient algorithm to solve for the electron wave-functions and the ionic relaxation, as well as an integration over short time scales, which otherwise would dominate the evolution of the system toward an energy minimum [68].

The entire approach is commonly referred to as 'first-principles' or 'ab initio' calculations since it does not rely on any parameters that need to be specified by comparison to experiment. Any parameters that enter in the calculations (other the fundamental constants e, $\hbar$, m_e and the charges and masses of the ions), can be specified by theoretical considerations in a self-consistent manner. The only important approximation is the expression for the exchange-correlation functional, at the LDA or the GGA level. Despite this ad-hoc approximation, the application of these methods to the study of solids, molecules and clusters has been remarkably successful [69].

It is appropriate to remark here on an altogether different limitation of this approach, and to address a misconception regarding the effect of this limitation on total-energy calculations. As was shown by the seminal work of Hybertsen and Louie [70], and Godby, Schlüter and Sham [71], density functional theory cannot describe accurately the energy spectrum of quasi particles that correspond to excitations of the many-electron system. This fundamental limitation is due to density functional theory itself and has nothing to do with the approximations involved in the exchange-correlation functional (LDA or GGA). One well known consequence of this limitation is that DFT calculations give a band gap for semiconductors that is off by a large percentage (often -50% to -100%). However, this limitation of DFT does not affect total-energy calculations. The reason is the following: there are two types of excitations in a system of ions and electrons above its true ground state: (a) Excitations due to changes in the positions of the ions; for each such configuration of the ions the electrons are in the corresponding Born–Oppenheimer ground state. (b) Excitations of the electronic degrees of freedom at a *fixed* ionic configuration, above the electronic ground state. DFT at the LDA or GGA level provides a very satisfactory description for type (a) excitations but not for type (b) excitations; that is, energy differences from the true ground state due to motion of the ions with the electrons in the instantaneous Born–Oppenheimer surface, are very well represented by DFT/LDA or GGA calculations. This is the type of excitation involved in most MD simulations and in particular those relevant to semiconductor growth phenomena. Type (b) excitations are not dominant in these problems. In our experience, for most cases

Table 1
Comparison of computational cost of different atomistic approaches

	ab initio (DFT/LDA, GGA)	Tight-binding	classical potentials
Code size (lines)	10^4	10^3	10^2
Basis set size	100–500	4	
CPU time/MD step	1 h	1 min	1 s
Physical time/MD step	1 fs	1 fs	1 fs

In all cases order-of-magnitude estimates are given. The code size corresponds to the part that calculates the energy and forces in each approach, excluding the part that performs molecular dynamics, which should be common to all approaches. The basis set in the ab initio simulations is assumed to be plane waves; the two sizes quoted correspond to the number of plane waves needed for converged calculations for Si or C. For the tight-binding approximation, we assume sp^3 type elements, with four orbitals per atom. For CPU time estimates, a system of 250 Si atoms is assumed to be simulated on a modern workstation with a rating of 100 Mflops.

where accurate dynamics and relative energies are important, DFT/LDA or GGA calculations are indeed a useful and accurate tool for obtaining a realistic description of the physical system.

3. Comparison of computational approaches

A comparison of the three major approaches described above(classical interatomic potentials, tight-binding approximation and first-principles calculations) in terms of the computational cost for studying a typical structure of interest is given in Table 1. We assume that the system of interest has a size equivalent to 250 times the atomic volume of a Si atom, with periodic boundary conditions. This is a model large enough for studying typical surfaces in a slab geometry, or clusters (we make the distinction between volume of the system and actual number of atoms, because the former determines the size of basis functions in a plane wave basis for DFT calculations).

One measure of the computational complexity is the effort involved in developing the computer code for each method (assumed to be roughly proportional to the size of the code). Other measures include a typical number of basis functions needed for a converged calculation (for illustration, we assume a plane wave basis in the first-principles approach) and the cost per time step in a molecular dynamics simulation. To estimate the latter, we assume that a typical medium-range modern workstation is used, with a CPU specification of order 100 Mflops and adequate memory to handle the computation without excessive paging (256 MB). Obviously, the simulations based on the classical potentials are much less costly than either the tight-binding or the first-principles calculations. Interestingly, the physical time to which each time step in a MD simulation would correspond is essentially the same for all three approaches, of order 1 fs.

It is worthwhile to contemplate the limitations of these approaches. Although a system equivalent in size to 250 Si atoms (as the one used in the above estimates) may seem somewhat limited, it is actually adequate to describe a wide range of important processes, including many interesting cases of bulk or surface diffusion. With modest increases in system size (a factor of two or three) it is even possible to describe some of the most complicated structures such as the (7×7) dimer-adatom-stacking fault reconstruction of Si(111) [72], or diffusion around steps on the Si(100) surface [73]. While these sizes exceed only by a small factor the sizes which could be handled by modern workstations, the increase in computational cost is large enough so that at present such calculations can only be handled by supercomputers, based on vector processing or parallel architectures. Much effort is being devoted at present toward developing new algorithms that will scale efficiently with system size. The computational cost of typical algorithms in current use scales roughly as the third power of the system size (this is referred to as $O(N^3)$ scaling, where N is a measure of the system size such as the number of atoms or number of valence electrons). It is hoped that the new algorithms will achieve $O(N)$ scaling, which will make it possible to treat considerably larger systems. Most of these methods are still in the developing stage and we refrain from discussing them in any detail. Assuming that the $O(N)$ efforts will be crowned with success, it appears that the bottle-neck in realistic simulations will still be the extremely short time scale for which simulations can be performed, be-

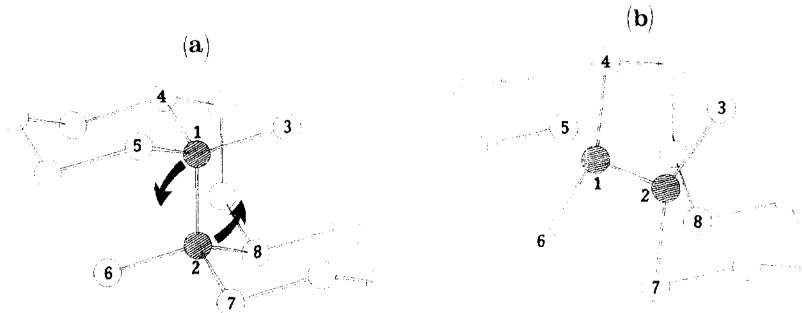

Fig. 1. Illustration of the atomic motion in the concerted exchange mechanism for self-diffusion in Si. The pair of exchanging atoms, labeled 1 and 2, is shown shaded; their immediate neighbors are labeled 3–8. (a) The equilibrium configuration; the arrows indicate the directions in which the two atoms move away from the equilibrium, toward the saddle point-configuration. (b) The saddle-point configuration; the pair of exchanging atoms as well as two of their immediate neighbors (5 and 8) are three-fold coordinated. Notice that in addition to bond breaking, there is also new bond formation, between the exchanging atoms and certain neighbors (1–6 and 2–3).

cause each step in the simulations corresponds to a very small physical time interval (see Table 1).

A more interesting comparison of the different approaches is in terms of the degree of realism with which they represent true physical systems. It is evident that the short cuts made in the name of computational speed in the classical potential and the tight-binding approaches, will result in a certain cost of realism. The question arises, How can one make *quantitative* comparisons of the relative degree of realism embodied in the different approaches? This is not a simple question, since few systems have been examined in detail with all the available approaches.

Much effort has been expended in determining the accuracy of Si classical potentials by comparing their

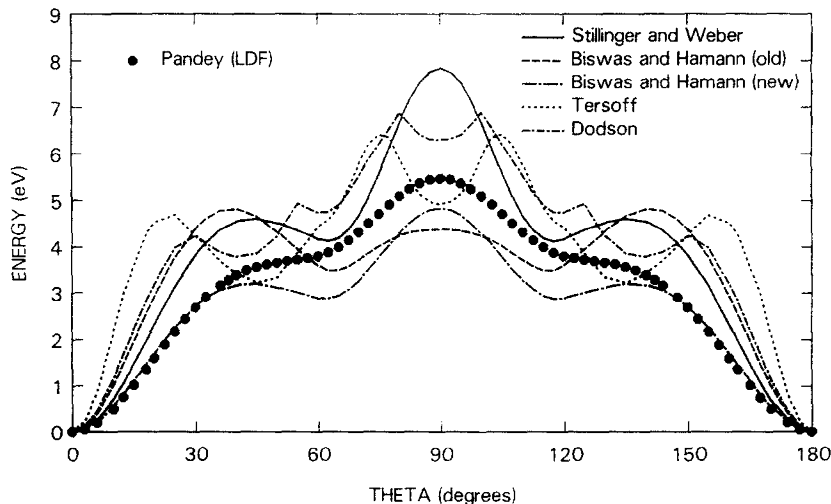

Fig. 2. Total energy along the concerted exchange path, as calculated from first-principles calculations (dots, labeled Pandey (LDF) [74] and various classical potentials (lines, labeled by author, see text and corresponding references; the words 'old' and 'new' refer to earlier and more recent versions of the Biswas–Hamann potential; the earliest parametrization was used for the Tersoff potential). The path is shown in terms of one of the two angular variables involved in the exchange, the polar angle θ. No atomic relaxation is allowed in this comparison so that the atomic configurations used in the various approaches are identical.

predictions for structures to which they had not been fitted, and for which first principles results exist. Most of this effort has focused on comparing different bulk phases of Si, or static configurations, such as the optimal structure of semi-infinite or finite systems (surfaces or clusters). While these studies are very useful, the problem of semiconductor growth imposes rather more stringent requirements on the computational approach. Namely, since growth is an inherently non-equilibrium phenomenon, it is desirable that the computational approach reproduce not only equilibrium structures and their relative energies, but also saddle-point configurations and their energy relative to the neighboring stable and metastable configurations. We are aware of two studies that attempt such comparisons between different computational approaches, which we review next.

The first such study deals with a mechanism for self diffusion in bulk Si [42]. Several self diffusion mechanisms have been discussed in the literature: the two most prominent involve defects such as vacancies and interstitials; the third, proposed by Pandey [74], is based on a complicated atomic motion that allows two atoms to exchange positions without the presence of defects. The latter mechanism, referred to as the 'concerted exchange mechanism', includes a wide variety of local structures in which the two atoms that are exchanging positions have three-fold or four-fold coordination while covalent bonds to their neighbors are being broken or formed, as indicated in Fig. 1. This sequence of bond breaking and formation is also relevant to surface growth phenomena. In Fig. 2 we compare the energy along the concerted exchange path as given by the first-principles calculations of Pandey and by classical potentials of the Stillinger–Weber or the Tersoff type. In both cases, there are serious discrepancies between the classical potential results and those of the more reliable first-principles calculations. One important discrepancy is the large difference in the energy of the saddle point(the mid point of the path), which corresponds to the activation energy for this process. A second important discrepancy is the existence of deep metastable minima in the classical potential results, which are absent from the first-principles results; such features in the energy landscape would lead to false dynamics and could trap a simulation in an artificially stable but irrelevant structure. In some sense, the test described above is one of the most stringent ones that can be envisioned, since most of the configurations are very far removed from the data bases used to construct the classical potentials. These configurations, however, are the most interesting ones because they correspond to local distortions relevant to surface diffusion and growth phenomena.

The second detailed comparative study concerns diffusion on the Si(100) surface. Since most of the Si wafers for electronic device applications have the (100) surface exposed, on which any subsequent growth or interface formation takes place, understanding diffusion and growth phenomena on this surface is evidently very important. Investigations of diffusion mechanisms on this surface have been reported, using classical potentials (both the Stillinger–Weber [75,76] and the Tersoff one [77,78]) as well as first-principles calculations [79]. A recent detailed comparison of the classical potential results to a more thorough first-principles calculation was provided by Jonsson and coworkers [80]. In that work, DFT/LDA and GGA calculations are reported, using stricter convergence criteria, more extensive relaxation of the substrate and a denser grid to map the motion of Si adatoms on the Si(100) substrate than in earlier work. Some interesting observations emerge when the results of the different approaches are compared.

Essentially all of the *specific* features of the energy landscape associated with the motion of a single Si adatom on the Si(100) surface obtained from the classical potential calculations are in disagreement with the results of the first-principles calculations. This includes the position of local minima (the stable and metastable configurations) as well as the saddle points. The disagreement is not surprising, since the motion of the adatom on the surface involves rather complex bonding geometries with extensive rehybridization, which can only be captured through a quantum mechanical treatment of the electronic degrees of freedom. Thus, the classical potential calculations cannot be expected to give a realistic description of atomic motion on the Si(100) surface. There is one general feature of the energy landscape which the classical potential results reproduce adequately, that is, the highly anisotropic barriers for diffusion. Specifically, diffusion along the

dimer rows, either on top of them or in the troughs between them, is faster than perpendicular to the dimer rows. This is also in agreement with experiment [2]. This feature, together with the result that a substantial amount of deposited atoms land on top of the dimer rows, has been invoked by Metiu and coworkers to predict certain aspects of the initial stages of growth on this surface [75]. These predictions, which are relevant to recent observations on the initial stages of growth [81–83], are an example of how classical potentials can be used to produce a qualitatively interesting picture, despite their shortcomings.

Actually, there is disagreement in certain important aspects even between the results of earlier and more recent first-principles calculations for Si adatom diffusion on the Si(100) surface. Specifically, the calculation of Brocks, Kelly and Car [79] reported a lowest-energy diffusion path for the single Si adatom on Si(100) which involves hoping onto the dimer row and back down again, whereas the calculation of Jonsson and collaborators [80] reported a lowest-energy diffusion path exclusively within the troughs between dimer rows. These two paths are illustrated in Fig. 3, with the S–H–D–H–S path suggested in Ref. [79], and the S–T–S path suggested in Ref. [80]. The two calculations are based on exactly the same methodology, that is DFT/LDA, with non-local pseudopotentials, in a supercell with repeated slabs separated by vacuum regions, and using a plane wave basis; they differ in the density of grid points at which the energy landscape was evaluated, the number of plane waves and the degree of relaxation of the substrate. Apparently, these differences are significant enough to produce a substantially different diffusion path, which can have important implications in understanding the initial stages of growth on this surface. In particular, diffusion on top of the dimer rows has been invoked as an important process to explain the island shape anisotropy [75]. This scenario may have to be modified if the lowest-energy diffusion path does not involve the hopping of adatoms onto the dimer rows, as Jonsson and coworkers suggested [80].

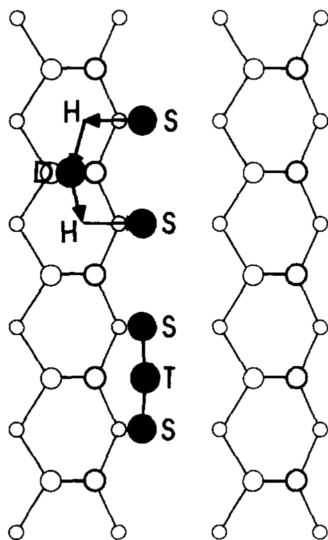

Fig. 3. Two possible paths for diffusion of a single Si adatom (shown shaded) on the Si(100) surface. The surface has the tilted dimer (2 × 1) reconstruction (notice the asymmetric dimers, with the higher atom indicated by a bolder open circle). The two paths concern diffusion along the dimer rows and were suggested by two independent first-principles calculations (S–H–D–H–S path: Ref. [79], S–T–S path: Ref. [80]. The notation follows that of Ref. [80].

4. Discussion and conclusions

Based on the preceding discussion we can comment now on the relative merits of the various approaches. The ease with which classical potential calculations can be performed presents a strong temptation for using these calculations to study complicated physical systems. One has to keep in mind though, that their accuracy is rather limited, and the results of these calculations can only be taken as a rough guide of what is physically plausible. This may or may not be helpful: physically plausible events can often be guessed by intuition, while not all the processes revealed by classical potential calculations are physically correct. Nevertheless, when these results address a generic rather than a very specific question, they probably give reasonable answers. In the present context, a generic question would be, for instance, the order of magnitude of the energy barrier for the concerted exchange mechanism, which most classical potentials give in the range of 5 ± 2 eV (see Fig. 2). Another generic question would be the anisotropy in diffusion on the

Si(100) surface, which the classical potentials also answer successfully. It is unrealistic, however, to expect that the classical potential calculations will provide the exact barrier for such a complex process as the concerted exchange mechanism, or the exact diffusion path for adatoms on such a complicated system as the Si(100) dimerized surface.

There is a different context in which classical potential calculations can be very useful. This concerns situations where one is interested in average properties, in a statistical mechanical sense, where an approximate energy comparison is adequate to produce reasonable sampling. An interesting application of this type has been reported by Kelires and Tersoff [19], who studied the ordering of Ge in Si/Ge structures on Si(100) substrates, using the Tersoff classical potential. They found intriguing ordering patterns which account successfully for experimental observations. The ordering is due to the strain pattern induced by the surface reconstruction on the substrate. Since the potentials were designed to reproduce well the elastic energy in this system, the Kelires–Tersoff calculation represents a judiciously chosen and successful application of classical potentials.

In short, one may use two rules of thump for judging the relevance of classical potential calculations:

(1) The calculation must involve atomic configurations which are reasonably close to the database used to determine the potential. An example where this rule was satisfied is the case of ordering in the Si/Ge system discussed above. A counter example where the rule is substantially violated is the case of Si adatom diffusion on the Si(100) surface.

(2) The calculation must address a question of generic rather than specific nature. Examples include order-of-magnitude estimates of different activation energies, inquiries into the presence or absence of anisotropy in dynamical processes, etc. Questions of this type can often be answered by intuition, but the classical potential calculations may serve to reinforce intuitive arguments and place limits on certain key quantities.

If neither of these rules apply, the relevance of these calculations to real physical situations may be questionable.

As far as first-principles DFT/LDA or GGA calculations are concerned, a certain degree of caution is also warranted when using their results to understand the behavior of real physical systems. As discussed earlier, two different calculations with exactly the same methodology can give answers that may lead to qualitatively different conclusions. For this reason, a thorough and exhaustive calculation of the type reported by Jonsson and coworkers [80] for Si adatom diffusion on Si(100) is needed to clarify the details of the microscopic mechanisms. When such studies are carried out, significant insight to real physical phenomena can be obtained. To our knowledge, there exist no blatant disagreements between the results of careful DFT/LGA or GGA calculations and experimental numbers (when these are available) or more elaborate calculations such as Quantum Monte Carlo or Configuration Interaction (when these are feasible), for covalently bonded systems. The occasional difference between results obtained with different exchange-correlation approximations (for example, differences between LDA and GGA results for the same physical system) is more a matter of refinement and gradual improvement, rather than an inherent limitation of the approach.

The advantages, then, of performing such computationally demanding calculations are two fold: First, in cases where experiment produces unexpected results that are not easily rationalized by simple arguments, these calculations can provide reliable comparisons that allow for a successful resolution of the puzzle (see for instance, the investigation of the surprisingly slow diffusion rate on the Ge(111)c(2 × 8) reconstructed surface [8]). Second, the first-principles calculations apply to a wide variety of physical situations and are not restricted to a model material such as Si. In contrast, empirical interactions are either grossly inaccurate when applied far from the data base from which they were constructed, and they are available for a very small number of materials (e.g. bulk C, Si, Ge, GaAs). Even for these materials, many years of intensive work has not produced a systematic improvement in the accuracy of the classical potentials.

To illustrate the effectiveness and reliability of the first-principles calculations, we discuss an example from our recent work on semiconductor growth phenomena: it concerns the case of group-V adsorbates acting as surfactants in Si epitaxy. The precise mech-

anism by which surfactants influence the mode of growth is still a matter of investigation and debate. Nevertheless, we have argued that a minimal requirement for the surfactant atoms is that they segregate easily during growth, otherwise they would lead to highly defective films [21,84]. Various elements have been tried as surfactants on Si, with the group-V elements As and Sb being the most successful. Surprisingly, while both As and Sb work well on the Si(100) surface, only Sb works well on the Si(111) substrate. This is difficult to explain without detailed knowledge of the surface structures involved. To this end, we have performed first-principles total-energy calculations for P, As and Sb overlayers on Si substrates, in all the allowed reconstructions. In the present context, an allowed reconstruction is one that renders the surface chemically stable, by making all group-V atoms three-fold coordinated and all substrate atoms four-fold coordinated. While only one reconstruction is allowed on the Si(100) substrate, consisting of group-V dimers, several possibilities exist for the Si(111) substrate: the group-V atoms can substitute for the top, bulk-terminated layer of Si atoms (forming a reconstruction with (1×1) periodicity), or they can form overlayers on top of the bulk-terminated Si layer consisting of trimers (with $(\sqrt{3} \times \sqrt{3})$ periodicity) or chains (with (2×1) periodicity). Of these reconstructions, according to our first-principles calculations, P and As prefer by a large margin the substitutional geometry, while Sb prefers either the trimer or chain geometry. All these findings are in agreement with experimental results [85–87].

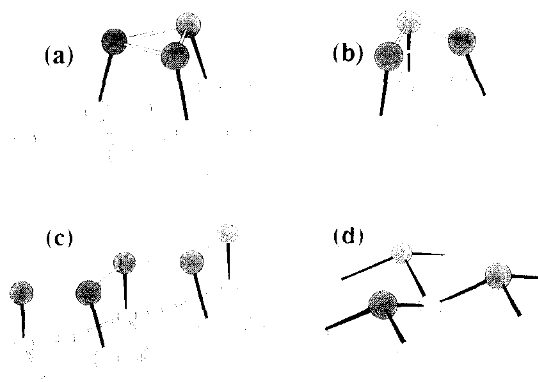

Fig. 4. Allowed reconstructions on the Si(111) surface, covered by group-V adsorbates (shown shaded). (a) Trimer reconstruction, with the trimer centers above hollow substrate sites (H_3 position) with $(\sqrt{3} \times \sqrt{3})$ periodicity. (b) Trimer reconstruction, with the trimer centers above second-layer substrate sites (T_4 position) with $(\sqrt{3} \times \sqrt{3})$ periodicity. (c) Chain reconstruction with (2×1) periodicity. (d) Substitutional reconstruction with (1×1) periodicity. The black bonds indicate bonds between adsorbate atoms and the substrate.

There is a significant qualitative difference between the various reconstructions of group-V atoms on Si(111): in the substitutional geometry every group-V atom is bonded to the substrate by three strong covalent bonds, all of which have to be severed so that the group-V atoms may float during growth. In contrast, only one strong covalent bond per group-V atom links the trimer or chain geometries to the substrate; the other two bonds of each group-V atom are to neighboring group-V atoms. This is illustrated in Fig. 4. Based on these observations, we predicted that Sb, which prefers the chain or trimer reconstructions, would act as a good surfactant on Si(111), since it can segregate easily by breaking only one covalent bond per adsorbate atom. In contrast, As or P, which prefer the substitutional geometry, would be poor surfactants. This has been verified by recent experimental work [88]. It is gratifying that even at this somewhat oversimplified level of theoretical consideration, the results of first-principles calculations can be a useful guide to experiment, predicting correctly the behavior of complex systems. In this example, the accuracy of first-principles calculations combined with their chemical specificity were essential in making the structural comparisons that are relevant to surfactant segregation.

In conclusion, we have provided a comparative study of various theoretical approaches that are employed in atomistic simulations of growth on semiconductors. We have discussed the main features of each approach and their advantages and disadvantages. We made suggestions for the conditions under which different approaches should be used, and pointed out the caveats involved in extracting information on the behavior of real physical systems.

Acknowledgements

This work was supported by the Office of Naval Research, Grant #N00014-95-1-0350.

References

[1] H. Ehrenreich, Science 235 (1987) 1029.

[2] Y.-W. Mo, B.S. Swartzentruber, R. Kariotis, M.B. Webb and M.G. Lagally, Phys. Rev. Lett. 63 (1989) 2393;
Y.W. Mo, J. Kleiner, M.B. Webb and M.G. Lagally, Phys. Rev. Lett. 67 (1991) 1998;
J.J. de Miguel, C.E. Aumann, R. Kariotis and M.G. Lagally, Phys. Rev. Lett. 67 (1991) 2830;
X. Chen, F. Wu, Z. Zhang and M.G. Lagally, Phys. Rev. Lett. 73 (1994) 850.

[3] B.S. Swartzentruber, Y.-W. Mo, R. Kariotis, M.G. Lagally and M.B. Webb, Phys. Rev. Lett. 65 (1990) 1913.
F. Wu, S.G. Jaloviar, D.E. Savage and M.G. Lagally, Phys. Rev. Lett. 71 (1993) 4190.

[4] Y.-W. Mo, D.E. Savage, B.S. Swartzentruber and M.G. Lagally, Phys. Rev. Lett. 65 (1990) 1020.

[5] X.-S. Wang, J.L. Goldberg, N.C. Bartelt, T.L. Einstein and E.D. Williams, Phys. Rev. Lett. 65 (1990) 2430;
J. Wei, X.-S. Wang, J.L. Goldberg, N.C. Bartelt and E.D. Williams, Phys. Rev. Lett. 68 (1992) 3885;
E.D. Williams and N.C. Bartelt, Science 251 (1991) 393;
E.D. Williams, Surface Sci. 299/300 (1994) 502;
E.D. Williams, R.J. Phaneuf, Jian Wei, N.C. Bartelt and T.L. Einstein, Surf. Sci. 294 (1993) 219.

[6] K. Takayangi, Y. Tanishiro, M. Takahashi and S. Takahashi, J. Vac. Sci. Techn. A 3 (1985) 1502; Surf. Sci. 164 (1985) 367.

[7] E. Ganz, S.K. Theiss, I.-S. Hwang and J. Golovchenko, Phys. Rev. Lett. 68 (1992) 1567;
I.-S. Hwang and J. Golovchenko, Science 258 (1992) 1119; Phys. Rev. Lett. 71 (1993) 255.

[8] E. Kaxiras and J. Erlebacher, Phys. Rev. Lett. 72 (1994) 1714.

[9] A.W. Denier van der Gon and R.M. Tromp, Phys. Rev. Lett. 69 (1992) 3519;
R.M. Tromp and M.C. Reuter, Phys. Rev. Lett. 68 (1992) 954, 820;
N.C. Bartelt, R.M. Tromp and E.D. Williams, Phys. Rev. Lett. 73 (1994) 1656.

[10] R.J. Phaneuf, N.C. Bartelt, E.D. Williams, W. Swiech and E. Bauer, Surf. Sci. 268 (1992) 227; Phys. Rev. Lett. 71 (1993) 2284;
N.C. Bartelt, J.L. Goldberg, T.L. Einstein, E.D. Williams, J.C. Heyraud and J.J. Metois, Rev. B 48 (1993) 15453.

[11] J. Sudijono, M.D. Johnson, M.B. Elowitz, C.W. Snyder and B.G. Orr, Surf. Sci. 280 (1993) 247.

[12] J. Villain, J. Phys. I (France) 1 (1991) 19;
I. Elkinani and J. Villain, Solid State Comm. 87 (1993) 105; J. Phys. I (France) 4 (1994) 949.

[13] M.D. Johnson, C. Orme, A.W. Hunt, D. Graff, J. Sudijono, L.M. Sander and B.G. Orr, Phys. Rev. Lett. 72 (1994) 116.

[14] R. Stumpf and M. Scheffler, Phys. Rev. Lett. 72 (1994) 254.

[15] F.K. LeGoues, Phys. Rev. Lett. 72 (1994) 876;
F.K. LeGoues, P.M. Mooney and J. Tersoff, Phys. Rev. Lett. 71 (1993) 396;
F.K. LeGoues, M. Copel and R. Tromp, Phys. Rev. Lett. 63 (1989) 1826;
F.K. LeGoues, V.P. Kesan and S.S. Iyer, Phys. Rev. Lett. 64 (1990) 40;
F.K. LeGoues, V.P. Kesan, S.S. Iyer, J. Tersoff and R. Tromp, Phys. Rev. Lett. 64 (1990) 2038.

[16] D.E. Jesson, S.J. Pennycook, J.-M. Baribeau and D.C. Houghton, Phys. Rev. Lett. 71 (1993) 1744;
D.E. Jesson, S.J. Pennycook and J.-M. Baribeau, Phys. Rev. Lett. 66 (1991) 750;
D.E. Jesson, S.J. Pennycook, J.-M. Baribeau and D.C. Houghton, Phys. Rev. Lett. 68 (1992) 2062;
D.E. Jesson, S.J. Pennycook, J.Z. Tischler, J.D. Budai, J.-M. Baribeau and D.C. Houghton, Phys. Rev. Lett. 70 (1993) 2293.

[17] A. Madhukar, Thin Solid Films 231 (1993) 8.

[18] A. Zunger and S. Mahajan, in: ed. S. Mahajan, Atomic Ordering and Phase Separation in Epitaxial III–V Alloys, Handbook on Semiconductors, Vol. 3 (Elsevier, 1994).

[19] P.C. Kelires and J. Tersoff, Phys. Rev. Lett. 63 (1989) 1164.

[20] M. Copel, M.C. Reuter, E. Kaxiras and R.M. Tromp, Phys. Rev. Lett. 63 (1989) 632.

[21] E. Kaxiras, Europhys. Lett. 21 (1993) 685.

[22] B.D. Yu and A. Oshiyama, Phys. Rev. Lett. 71 (1993) 585;
B.D. Yu and A. Oshiyama, Phys. Rev. Lett. 72 (1994) 3190.

[23] Z. Zhang and M.G. Lagally, Phys. Rev. Lett. 72 (1994) 693.

[24] A.-L. Barabasi, Phys. Rev. Lett. 70 (1993) 4102.

[25] M. Copel, M.C. Reuter, M. Horn von Hoegen and R.M. Tromp, Phys. Rev. B 42 (1990) 11682;
M. Horn-von Hoegen, F.K. LeGoues, M. Copel, M.C. Reuter and R.M. Tromp, Phys. Rev. Lett. 67 (1991) 1130;
J. Falta, M. Copel, F.K. LeGoues and R.M. Tromp, Appl. Phys. Lett. 62 (1993) 2962;
M. Copel and R.M. Tromp, Phys. Rev. Lett. 72 (1994) 1236.

[26] G. Meyer, B. Voigtlander and N.M. Amer, Surf. Sci. Lett. 274, L541 (1992);
B. Voigtlander and A. Zinner, Surf. Sci. Lett. 292, L775 (1993); J. Vac. Sci. Technol. A 12 (1994) 1932.

[27] M. Horn-von Hoegen, J. Falta, M. Copel and R.M. Tromp, Appl. Phys. Lett. 66 (1995) 487.

[28] G.S. Petrich, A.M. Dabiran, J.E. Macdonald and P.I. Cohen, J. Vac. Sci. Techn. B 9 (1991) 2150;
G.S. Petrich, A.M. Dabiran and P.I. Cohen, Appl. Phys. Lett. 61 (1992) 162.

[29] S. Iwanari and K. Takayanagi, J. Cryst. Growth 119 (1990) 229.

[30] H. Minoda, Y. Tanishiro, N. Yamamoto and K. Yagi, Surf. Sci. 287 (1993) 915.

[31] H. Nakahara and M. Ichikawa, Appl. Phys. Lett. 61 (1992) 1531.

[32] G.D. Wilk, R.E. Martinez, J.F. Chervinsky, F. Spaepen and J.A. Golovchenko, Appl. Phys. Lett. 65 (1994) 866.

[33] M.P. Allen and D.J. Tildesley, Computer Simulation of Liquids (Clarendon Press, Oxford, 1987).

[34] G.C. Abell, Phys. Rev. B 31 (1985) 6184.

[35] D.K. Choi, T. Takai, S. Erkoc, T. Halicioglu and W.A. Tiller, J. of Crystal Growth 85 (1985) 9;

H. Blamane, T. Halicioglu and W.A. Tiller, Phys. Rev. B 46 (1992) 2250.
[36] F.H. Stillinger and T.A. Weber, Phys. Rev. B 31 (1985) 5262.
[37] R. Biswas and D.R. Hamann, Phys. Rev. Lett. 55 (1985) 2001; Phys. Rev. B. 36 (1987) 6434.
[38] J. Tersoff, Phys. Rev. Lett. 56 (1986) 632; Phys. Rev. B. 37 (1988) 6991; 38 (1988) 9902.
[39] M.I. Baskes, Phys. Rev. Lett. 59 (1987) 2666.
[40] B.W. Dodson, Phys. Rev. B 35 (1987) 2795.
[41] K.E. Khor and S. Das Sarma, Phys. Rev. B. 36 (1987) 7733; 38 (1988) 3318.
[42] E. Kaxiras and K.C. Pandey, Phys. Rev. B 38 (1988) 12736.
[43] G.J. Ackland, Phys. Rev. B 40 (1989) 10351; 44 (1991) 3900.
[44] K.M. Glassford, J.R. Chelikowsky and J.C. Phillips, Phys. Rev. B. 43 (1991) 14557.
[45] B.C. Bolding and H.C. Andersen, Phys. Rev. B 41 (1990) 10568.
[46] A.D. Mystriotis, N. Flytzanis and S.C. Farantos, Phys. Rev. B 39 (1989) 1212.
[47] W.A. Harrison, Electronic Structure and the Properties of Solids (Freeman, San Francisco, 1980), and references therein.
[48] D.J. Chadi, Phys. Rev. B 29 (1984) 785.
[49] O.L. Alerhand and E.J. Mele, Phys. Rev. B 35 (1986) 1.
[50] D. Tomànek and M.A. Schlüter, Phys. Rev. Lett. 56 (1986) 1055; 36 (1987) 1208.
[51] F.S. Khan and J.Q. Broughton, Phys. Rev. B 39 (1989) 3688.
[52] A.P. Sutton, M.W. Finnis, D.G. Pettifor and Y. Ohta, J. Phys. C 21 (1988) 35R;
L. Goodwin, A.J. Skinner and D.G. Pettifor, Erophys. Lett. 9 (1989) 701.
[53] M. Menon and K.R. Subbaswamy, Phys. Rev. B 47 (1993) 12754.
[54] J.L. Mercer, Jr. and M.Y. Chou, Phys. Rev. B 49 (1994) 8506.
[55] R.E. Cohen, M.J. Mehl and D.A. Papaconstantopoulos, Phys. Rev. B 50 (1994) 14694.
[56] P. Blaudeck, Th. Frauenheim, D. Porezag, G. Seifert and E. Fromm, J. Phys.: Condens. Matter C4 (1992) 6389.
[57] C.Z. Wang, K.M. Ho and C.T. Chan, Phys. Rev. Lett. 70 (1993) 611.
[58] E. Kaxiras and Z. Guo, Phys. Rev. B 49 (1994) 11822.
[59] P. Hohenberg and W. Kohn, Phys. Rev. B 136 (1964) 864.
[60] W. Kohn and L.J. Sham, Phys. Rev. A 140 (1965) 1133.
[61] D.M. Ceperley and B.J. Alder, Phys. Rev. Lett. 45 (1980) 566;
J. Perdew and A. Zunger, Phys. Rev. B 23 (1981) 5048.
[62] J.P. Perdew, Proc. of the 21st Ann. Int. Symp. on Electronic Structure of Solids (Dresden, 1991);
J.P. Perdew and Y. Wang, Phys. Rev. B 33 (1986) 8800.
[63] B. Hammer, K.W. Jacobsen and J.K. Norskov, Phys. Rev. Lett. 70 (1993) 3971.
[64] Y. Juan and E. Kaxiras, Phys. Rev. B 48 (1993) 14944.
[65] W.E. Pickett, Comput. Phys. Rep. 9 (1989) 115.
[66] M.L. Cohen and J.R. Chelikowsky, Electronic Structure and Optical Properties of Semiconductors (Springer, New York, 1989).
[67] R. Car and M. Parrinello, Phys. Rev. Lett. 55 (1985) 2471.
[68] M.C. Payne, M.P. Teter, D.C. Allan, T. Arias and J.D. Joannopoulos, Rev. Mod. Phys. 64 (1992) 1045.
[69] R.O. Jones and O. Gunnarson, Rev. Mod. Phys. 61 (1989) 689.
[70] M. Hybertsen and S. Louie, Phys. Rev. Lett 55 (1985) 1418; M. Hybertsen and S. Louie, Phys. Rev. B 34 (1986) 5390.
[71] R. Godby, M. Schlüter and L. Sham, Phys. Rev. Lett. 56 (1986) 2415; B 37 (1988) 10159.
[72] K.D. Brommer, M. Needels, B.E. Larson and J.D. Joannopoulos, Phys. Rev. Lett. 68 (1992) 1502;
I. Stich, M.C. Payne, R.D. King-Smith, J.S. Lin and L.J. Clarke, Phys. Rev. Lett. 68 (1992) 1351;
K.D. Brommer, M. Galvan, A. Dal Pino, Jr. and J.D. Joannopoulos, Surf. Sci. 314 (1992) 57;
I. Stich, K. Terakura and B.E. Larson, Phys. Rev. Lett. 74 (1995) 4491.
[73] Q.-M. Zhang, C. Roland, P. Boguslawski and J. Bernholc, Phys. Rev. Lett. 75 (1995) 101.
[74] K.C. Pandey, Phys. Rev. Lett. 57 (1986) 2287.
[75] Z. Zhang, Y.T. Lu and H. Metiu, Surf. Sci. 80 (1991) 1248; Phys. Rev. B 46 (1992) 1917.
[76] C. Roland and G.H. Gilmer, Phys. Rev. Lett. 67 (1991) 3188; Phys. Rev. B 46 (1992) 13428; 46 (1992) 13437.
[77] D. Srivastava, B.J. Garrison and D.W.Brenner, Phys. Rev. Lett. 63 (1989) 302; Phys. Rev. B 47 (1993) 4464.
[78] J. Wang and A. Rockett, Phys. Rev. B 43 (1991) 12571.
[79] G. Brocks, P.J. Kelly and R. Car, Phys. Rev. Lett. 66 (1991) 1729.
[80] A.P. Smith, J.K. Wiggs, H. Jonsson, H. Yan, L.R. Corrales, P. Nachtingall and K.D. Jordan, J. Chem. Phys. 102 (1995) 1044.
[81] Z. Zhang, F. Wu, H.J.W. Zandvliet, B. Poelsema, H. Metiu and M. Lagally, Phys. Rev. Lett. 74 (1995) 3644.
[82] P.J. Bedrossian, Phys. Rev. Lett. 74 (1995) 3648.
[83] R.A. Wolkow, Phys. Rev. Lett. 74 (1995) 4448.
[84] E. Kaxiras, Mater. Sci. Eng. B 30 (1995) 175.
[85] F. Boszo and Ph. Avouris, Phys. Rev. B 43 (1991) 1847.
[86] R.S. Becker, B.S. Swartzentruber, J.S. Vickers, M.S. Hybertsen and S.G. Louie, Phys. Rev. Lett. 60 (1988) 116;
M. Copel, R.M. Tromp and U.K. Köhler, Phys. Rev. B 37 (1988) 10756;
M. Copel and R.M. Tromp, Phys. Rev. B 37 (1988) 2766.
[87] P. Martensson, G. Meyer, N.M. Amer, E. Kaxiras and K.C. Pandey, Phys. Rev. B 42 (1990) 7230.
[88] M. Horn-von Hoegen, J. Falta, M. Copel and R.M. Tromp, Appl. Phys. Lett. 66 (1995) 487.